Si atom adsorption and diffusion on Si(110)-(1×1) and (2×1)

Veronika Brázdová* and David R. Bowler†
London Centre for Nanotechnology, UCL, 17-19 Gordon Street, London WC1H 0AH, United Kingdom;
Department of Physics and Astronomy, UCL, Gower Street, London WC1E 6BT, United Kingdom;
and TYC@UCL, Gower Street, London WC1E 6BT, United Kingdom
(Received 6 November 2009; revised manuscript received 17 February 2010; published 29 April 2010)

We present a systematic periodic density-functional study of Si adsorption and diffusion on the Si(110)-(1×1) and (2×1) surface. The most stable binding configurations on both reconstructions are with a threefold coordinated adatom bridging the gap between two surface zigzag rows. Several of the structures can be stabilized by a lateral shift of the rows or by distortion of a row. The different structures can be identified from their density of states and scanning tunnel microscopy/current image tunneling spectroscopy (STM/CITS) images. Diffusion on the (1×1) surface is equally likely to proceed along and across zigzag rows. Along rows either simple diffusion or an exchange mechanism can occur, across rows only an exchange mechanism is possible. Diffusion on the (2×1) reconstruction is easier in the direction along rows than across and proceeds as simple diffusion, not exchange. The mobility of the adatom is higher on the (2×1) reconstruction.

DOI: 10.1103/PhysRevB.81.165320 PACS number(s): 31.15.ae, 31.15.es

I. INTRODUCTION

Silicon has been immensely important in condensed-matter physics, surface science, and industrial applications for 50 years or more. The Si(001) and Si(111) surfaces have been intensively studied. By contrast, Si(110) has been less intensively investigated.

The Si(110) surface has potential applications in semiconductor technologies and in surface science due to its high hole mobility compared to the Si(100) surface[1] in complementary metal-oxide semiconductor (CMOS) transistors. There is also interest in SiGe and semiconductor-on-insulator devices on Si(110), which requires a good understanding both of diffusion on the surface and of surface structures. Recent developments in CMOS transistor technology [e.g., FinFETs and structures grown by patterned atomic-layer epitaxy (ALE)] are either grown on or create Si(110) surfaces.[2,3] Understanding Si adatom diffusion is important for engineering the growth of the surface.

The Si(110) surface is not like III-V semiconductor surfaces, which have zigzag chains and show a simple buckling (1×1) relaxation where alternate atoms rise and fall; the native terminated surface shows the same chains which can relax in either (1×1) or (2×1) patterns (depending on how the buckling is arranged from chain to chain). However, in experiment, the Si(110) surface has a complicated reconstruction at room temperature, usually described as (16×2),[4–7] with other periodicities occasionally being observed and a high temperature (16×2)↔(1×1) transition reported.[8] The (16×2) reconstruction consists of alternating raised and lowered stripes ~25.1 Å wide,[9] running in the $[\bar{1}12]$ direction. The reconstruction has been studied with scanning tunnel microscopy (STM),[4–6,8–11] low-energy electron diffraction (LEED),[7] and photoemission spectroscopy[11,12] and various models for the structural features have been proposed,[8,10–14] but there is no conclusive agreement on the atomic positions of the reconstruction.[11]

There are various reasons for studying the (1×1) and (2×1) surfaces and the behavior of adatoms on these surfaces. First, the (16×2) reconstruction forms on top of the bulk zigzag chains and understanding how this reconstruction forms will be aided by a detailed knowledge of the diffusion and electronic structure of adatoms on the simple surfaces. The (1×1) and (2×1) reconstructions are therefore the ideal starting point for a systematic study of the Si(110) surface and the electronic structure of adatoms on these surfaces may give clues to what adatoms are found in the (16×2) reconstruction. Second, the structures grown by patterned ALE are expected to have (1×1) and (2×1) sidewalls. To understand how these structures will evolve during growth, the structure and diffusion of adatoms on these surfaces will be key.

The (1×1) and (2×1) reconstructions and the most stable adatom structures on these reconstructions have been studied with tight binding[15] and density functional theory (DFT).[13,16] There is, however, no study systematically investigating Si adsorption on these surfaces and none at all on Si diffusion. In this paper, we present DFT calculations of the atomic and electronic structure of Si adatoms on both surfaces, and calculate the barriers to diffusion between different adatom sites. After introducing the methods, we first present the stable adsorption sites for Si on the (1×1) and (2×1) reconstructions as well as a detailed analysis of their electronic structure. We then examine diffusion pathways on the surface and conclude with a comparison to Si adatom diffusion on Si(001).

II. METHODS

Density functional theory with the gradient-corrected Perdew-Burke-Ernzerhof (PBE) (Ref. 17) exchange-correlation functional, as implemented in the Vienna *Ab Initio* Package (VASP) code[18,19] was used. The core electrons were described by the projector augmented-wave (PAW) method.[20,21] The plane-wave basis set kinetic energy cutoff was set to 250 eV. The Brillouin zone was sampled using Monkhorst-Pack grids.[22] Gaussian smearing was used for fractional occupancies, with a 0.01 eV width. The conver-

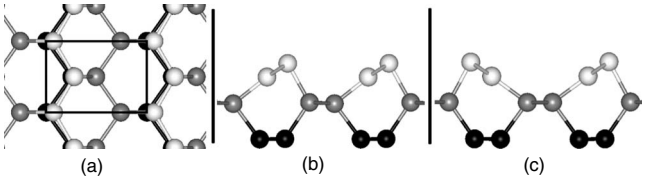

FIG. 1. (a) Top view of the (1×1) reconstruction with the surface unit cell marked. (b) Side view of the top layers of the (1×1) reconstruction. (c) Side view of the top layers of the (2×1) reconstruction.

gence criterion for forces on atoms was 0.01 eV/Å and for total energy 10^{-6} eV. This setup leads to the relative energies and energy barriers being reliable to 10^{-2} eV. The projected density of states was evaluated with the small (0.01 eV) smearing and convoluted with a Gaussian curve of 0.1 eV width in post-processing. STM and current image tunneling spectroscopy (CITS) images were simulated using the Tersoff-Hamann approach.[23]

The transition state search was done using the climbing image nudged elastic band (NEB) method as implemented in the VTST code.[24,25] The climbing image modification of NEB has been shown to converge rigorously to the highest saddle point.[24] For all apart from one search, we used one image, which is functionally equivalent to the dimer method[26] with a very small spacing or the force inversion method.[27] This has recently been shown[28] to yield extremely accurate energy barrier values (though the detailed shape of the barrier is not found). For the exchange mechanism across zigzag rows on the (1×1) reconstruction, we used four images.

The Si crystal cell was optimized by fitting the total energy/volume curve with the Murnaghan equation. The resulting lattice parameter is 5.47 Å, which differs by 0.7% from the experimental value of 5.431 Å.[29,30] This translates into optimized surface cell parameters of $a=5.47$ Å and $b=3.86$ Å for the Si(110) surface. In this work, we use a (4×4) surface unit cell with corresponding lattice parameters, $a=21.87$ Å and $b=15.47$ Å, with a $(2\times3\times1)$ k-point mesh. With this k-point mesh, relative energies of the different structures are converged. The lattice parameter perpendicular to the surface was set to 35 Å, which results in ~14.5 Å of vacuum between the periodic images of the slab. The slab contained 11 Si atomic layers and was terminated with hydrogen atoms at the bottom. With 11 Si layers, the forces on the atoms in bulk positions in the middle of the bulk-cut slab are smaller than 10^{-2} eV/Å. The bottom 5 Si layers were kept fixed at bulk positions; the rest of the structure was optimized.

III. RESULTS

A. The Si(110) surface

Each atomic layer in the [110] direction of bulk Si contains zigzag chains running along the $[1\bar{1}0]$ direction. The layers are arranged in AB stacking. At the (110) surface, the top layer buckles; all chains buckled in the same direction create the (1×1) reconstruction, alternately buckled chains the (2×1) reconstruction (see Fig. 1). The layer is thus effectively split into two layers, which are 0.74 and 0.75 Å apart for the (1×1) and (2×1) reconstructions, respectively. There is minimal lateral movement of the atoms. Atoms in the layer below (depicted in gray in Fig. 1) remain virtually in bulklike positions.

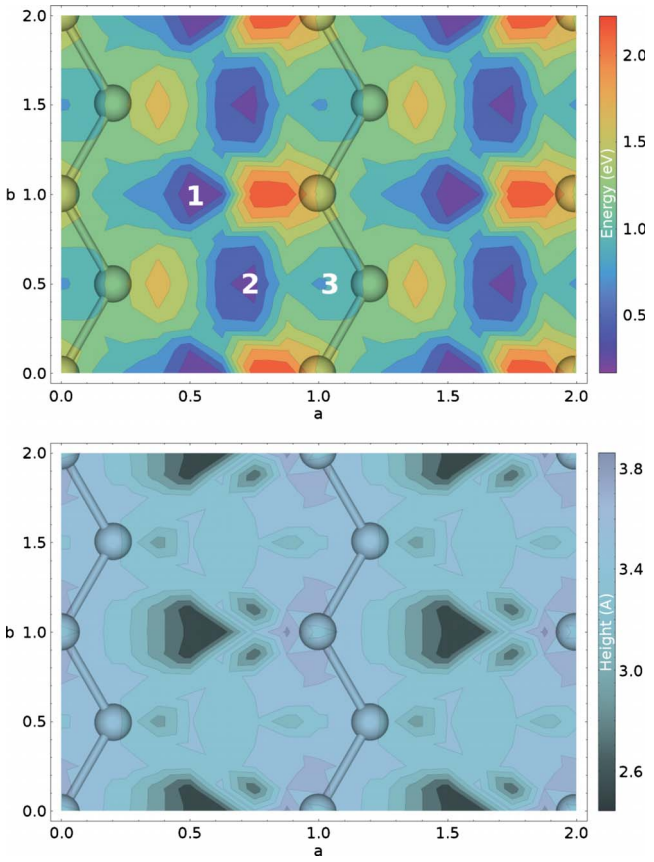

FIG. 2. (Color online) (Top) The Si(110)-(1×1) potential-energy surface for an adsorbed Si atom. The energy is relative to the total energy of the most stable structure with an adatom. (Bottom) Height of the adatom in the cell. The height is given with respect to the first bulklike layer of the surface. Only a (2×2) surface unit cell is shown for clarity in both plots.

With the exchange and correlation described by the PBE functional, the (1×1) reconstruction is 11 meV per a (2×1) unit cell more stable than the (2×1) reconstruction. Previous publications[13,16] report the (2×1) reconstruction as the more stable one. However, we find that the LDA functional, used in Refs. 16 and 13, gives the reversed stability order: according to our calculations, with LDA and standard VASP ultrasoft pseudopotentials or PAW potentials, the (2×1) reconstruction is 9 and 13 meV per a (2×1) unit cell more stable than (1×1), respectively. We note that relative energies and diffusion barriers described in Secs. III B and III D change only by a small amount with the LDA functional (e.g., the relative energy of structures 1-1 and 1-2c changes by 0.08 eV and the energy barrier for adatom diffusion between these two sites by 0.04 eV) and we have used PBE throughout.

We have taken care to converge our calculations with respect to Brillouin zone integration and plane-wave cutoff, and are confident that PBE shows (1×1) to be more stable

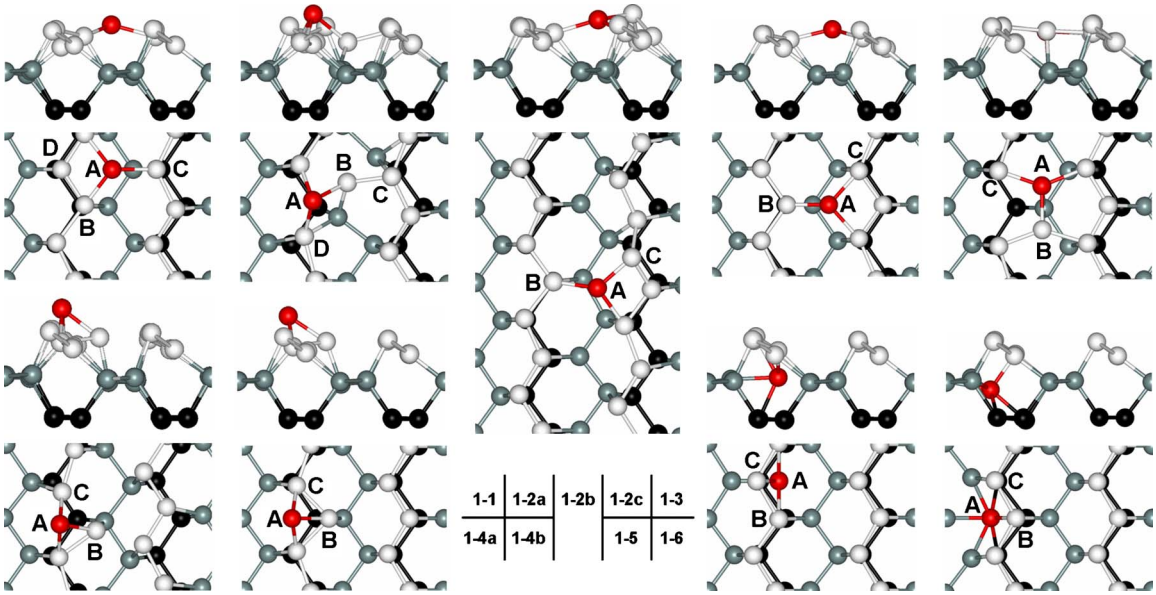

FIG. 3. (Color online) The most stable adsorption sites on the (1×1)-Si(110) surface.

than (2×1). However, the two relaxations are so close in energy that we investigate the behavior of adatoms on both reconstructions, and note that the exchange-correlation functional may have an effect on the band gap and influence the structure found to be more stable. A detailed investigation using more accurate methods (such as the GW approximation) would be required to find a definitive answer, which is beyond the scope of this study. However, both forms of buckling might be observed experimentally, particularly in small areas and when influenced by strain. The contrast to III-V semiconductor (110) surfaces is quite striking: the buckling and associated charge transfer is exclusively one way with the group V atoms buckling up and group III atoms buckling down, yielding only the equivalent of the (1×1) reconstruction.

B. Adsorption sites

1. Si adatom on the (1×1) *surface*

Figure 2 shows the potential energy surface (PES) of a Si adatom on the (1×1) surface. Each point in the plot was obtained by fixing the coordinates of the adatom in the *a* and *b* directions while allowing it to move in the direction perpendicular to the surface; we used eight points in the *a* and *b* directions, giving 64 points in the (1×1) cell. The surface was allowed to relax. The height of the adatom (Fig. 2, bottom) is within 2.5–3.7 Å above the first bulklike layer (the gray-colored layer in Fig. 1). For comparison, the top surface layer is 2.1 Å above this layer on the clean surface. In the fully optimized structures the adatom can be closer to the surface, but, in the most stable structures, is never below the first bulklike layer.

There are three regions in the (1×1) cell where the adsorbed atom will be stable. These appear as blue basins in Fig. 2. The most stable adsorption sites, found by fully optimizing the structures, are indeed in these three regions (Fig. 3, Table I).

The most stable site (1-1) is in basin number 1. The adatom is positioned between two zigzag rows and bound to two top-layer atoms and one second-layer atom in an sp^2-like configuration. Its height is the same as that of the topmost surface layer.

Another possibility is for the adatom to be bound to one top-layer atom and two second-layer atoms. This sp^2-like configuration (1-2c) occurs in basin 2 and the adatom is again at the height of the top surface layer. This structure is 0.34 eV less stable than 1-1 and can be stabilized by almost 0.2 eV in two different ways: if the adatom is shifted into basin 3 and one surface atom displaced into the gap between two rows (in between basins 1 and 2, a fairly stable position for an adatom in itself), the structure (1-2a) is stabilized by 0.18 eV. Alternatively, if one whole row is disturbed, the structure is stabilized by 0.17 eV (1-2b).

TABLE I. Si adsorption sites on the (1×1) surface. Energies in eV.

Site	E_{rel} [a]	E_b [b]
1-1	0.0[c]	−4.81
1-2a	0.16	−4.65
1-2b	0.17	−4.64
1-2c	0.34	−4.47
1-3	0.44	−4.37
1-4a	0.50	−4.31
1-4b	0.70	−4.11
1-5	1.64	−3.17
1-6	1.96	−2.85

[a]Total energy difference with respect to the most stable configuration.
[b]Binding energy with respect to the clean (1×1) surface and a gas phase Si atom.
[c]Reference energy.

Structure 1-3, 0.44 eV less stable than 1-1, is a variation of 1-2a: one surface atom is displaced into the space between rows and the adatom forms a dimerlike structure with it. Both are fourfold coordinated, each with one bond to the third surface layer.

In 1-4a we see another example of stabilization of a structure (1-4b) by moving a surface atom from its position, as in the case of 1-2a. The complex is stabilized by 0.20 eV, which is comparable to the 0.17 eV stabilization of 1-2a. We can also consider structure 1-2a as a stabilized variant of both 1-4a and 1-4b, with the adatom closer to the surface. The structures 1-4a and 1-4b are ones where the adatom is furthest away from the surface, and they are also the least stable, except for structures with interstitial adatoms. These (1-5 and 1-6) are 1.64 and 1.96 eV less stable than 1-1 and we will therefore not consider them further.

Adsorption of silicon on silicon surfaces typically shows a competition between passivating dangling bonds at the surface and the strain induced by forming new bonds on an existing reconstruction or relaxation. This competition is clearly seen here: the adatoms form three bonds to surface atoms, but the bond lengths and angles are far from the ideal bulk values. Most of the lowest-energy structures consist of the adatom bonding to a relatively undisturbed surface, with the strain being absorbed by the adatom itself. These structures follow what might be expected on the basis of simple bonding, with the adatom bonding to two atoms on one zigzag row and one on the other. However, structures such as 1-2a and 1-3 show considerable rearrangement of the surface, showing that the (1×1) has complex behavior (as is seen in the formation of large-scale reconstructions).

2. Si adatom on the (2×1) surface

On the (2×1) surface, the adatom is most stable when it connects two zigzag rows by binding to one top layer atom of one row and two of the other (2-1, Fig. 4, Table II). The two rows are pulled toward the adatom. The surface atom C has gained a bond in the direction of its original dangling bond. The adatom is above the surface, in a nonplanar configuration that is closer to the sp^3 geometry of the bulk than sp^2.

The other stable structure, 2-2, is by 0.37 eV less stable than 2-1. The adatom is bound to the second surface layer, connecting two zigzag rows. The surface atoms to which it binds are pulled upwards, almost to the level of the top surface layer, but not laterally. The adatom has an sp^2-like configuration; since the surface has only two stable sites and is less stable energetically, we did not create a potential energy surface. We also found two interstitial binding sites (2-3 and 2-4), but as they are 1.86 and 3.00 eV less stable than 2-1, we will not consider them further.

The lack of flexibility in the (2×1) surface is quite striking: there are only two stable sites for the adatom, which conform to the expected pattern of two bonds to one zigzag row and one bond to another. There is no sign of the freedom to rearrange found on the (1×1) surface; we will return to this observation when considering diffusion.

3. Comparison

The most stable structures on both surfaces are those where a threefold-coordinated adatom is bound to one atom of a zigzag row and to two atoms of a neighboring row. The adatom bridges the gap between the rows, at the height of the second surface layer or higher. The binding energies[31] of the adatom at the two surfaces are also comparable (Tables I and II), although the adatom is slightly more strongly bound on the (2×1) reconstruction: −4.81 and −4.47 eV for 1-1 and 1-2c, respectively, and −4.97 and −4.60 eV for 2-1 and 2-2, respectively. Stabilization by deformation and shift of whole rows can also occur on both surfaces (structures 1-2a, 1-2b, and 2-1).

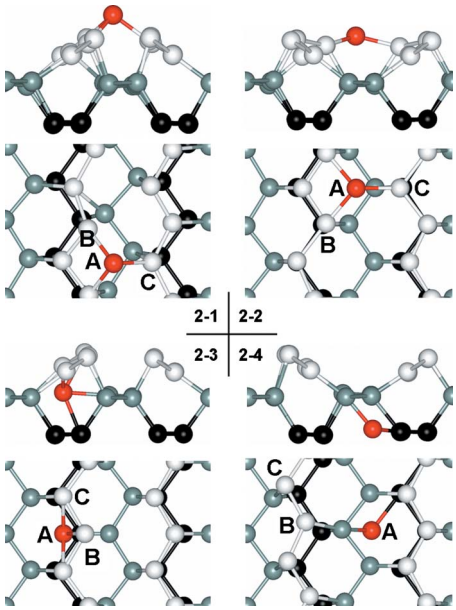

FIG. 4. (Color online) The most stable adsorption sites on the (2×1)-Si(110) surface.

There is no site on the (2×1) reconstruction that would allow a structure similar to 1-3 to be formed. An equivalent of the 1-4 structure on the (2×1) surface is a saddle point, not a minimum. The adatom is significantly less stable in interstitial binding sites than on the surface on both reconstructions [up to 2.0 and 3.0 eV less stable for (1×1) and (2×1), respectively]. The increased number of binding sites on the (1×1) surface is expected to increase the corrugation of the surface toward diffusion. Finally, we note that the addition of an adatom in the 2-1 site to the (2×1) surface

TABLE II. Si adsorption sites on the (2×1) surface. Energies in eV.

Site	E_{rel} [a]	E_b [b]
2-1	0.0[c]	−4.97
2-2	0.37	−4.60
2-3	1.86	−3.11
2-4	3.00	−1.97

[a]Total energy difference with respect to the most stable configuration.
[b]Binding energy with respect to the clean (2×1) surface and a gas phase Si atom.
[c]Reference energy.

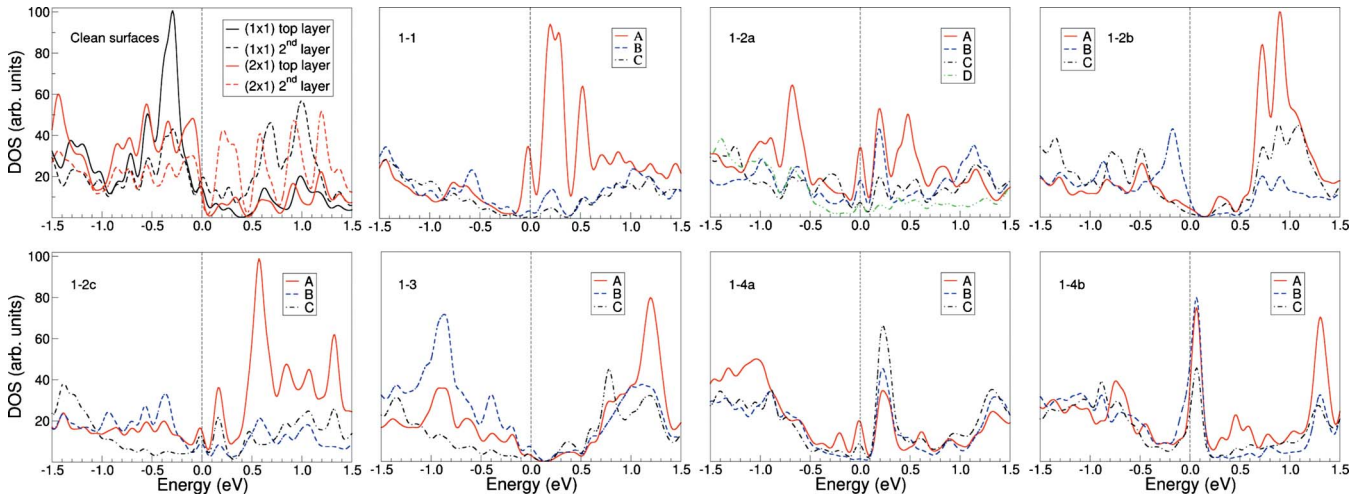

FIG. 5. (Color online) Density of states projected on atoms on the clean surfaces (top left) and at the different stable sites on the (1×1) reconstruction.

results in a *more stable* structure overall than the addition of an adatom in the 1-1 site to the (1×1) surface, though the stabilization is less than 10 meV per (2×1) cell. This indicates the extreme sensitivity of the (110) surface to local distortions.

C. Electronic structure

We now turn to the electronic structure of these adatoms, presenting both densities of states [which will be useful in comparison to scanning tunneling spectroscopy (STS) measurements and given information about the state of surface atoms] and simulated STM images for particular energy windows (which will correspond to CITS maps). It is important to state that DFT is not reliable for band gaps and that there is no physical significance to the eigenvalues. However, DFT-based simulated STM images often produce extremely good predictions of experimental images (though the bias voltage of empty state images often needs to be adjusted to account for the gap). We are therefore confident that the broad features of the density of states (DOS) should be observed in STS measurements, though the energies of unoccupied states might need adjusting; we also expect that the simulated STM images will correspond to experimental observations, which should give useful information when interpreting images of adatoms on Si(110) and understanding the large-scale reconstructions which are found on the surface.

1. The (1×1) *surface*

The DOS projected on atoms of the clean surfaces and of the structures with adatoms on the (1×1) reconstruction is plotted in Fig. 5. At the clean surface, both (1×1) and (2×1), the band gap is closed and the dangling bonds of the atoms of the top layer show as peaks close to the Fermi level. In contrast, atoms from the second layer are marked by peaks in the empty states.

The adatom significantly changes the electronic structure of the surrounding atoms. In 1-1 the DOS of the adatom has one small peak directly below the Fermi level and two large peaks just above the Fermi level. The peaks in the DOS of the neighboring (first surface layer) atoms are attenuated. Correspondingly, in simulated CITS images (Fig. 6), the adatom appears as a bright spot between two zigzag rows both in occupied and empty states. The atoms bound to it appear darker in comparison in occupied states. The bright spot is in between the two zigzag rows.

The 1-2c structure shows DOS similar to 1-1, with the most prominent adatom peaks in the empty states and smaller peaks on either side of the Fermi level. The bright spot in CITS images, caused by the adatom, is in line with one of the zigzag rows, in contrast to the CITS images of structure 1-1. In the occupied states, the adatom and atoms bound to it appear darker relative to the surrounding clean surface in 1-2c than in the case of 1-1.

Structures 1-2a and 1-2b each have a distinct DOS. The distortion of the zigzag rows can be seen in the CITS images of both. Note the shift of the zigzag row on the right side of the CITS images of 1-2a in empty states close to the Fermi level.

The adatom and its surrounding atoms in 1-3 do not show large peaks close to the Fermi level in their DOS and thus also appear as darker spots in occupied states and in empty states below $\sim$0.7 eV. Above 0.7 eV, the two atoms bridging the gap between the rows can be clearly seen.

The DOS of the adatom in 1-4a and 1-4b is similar, as are their CITS images. The main difference is the distortion of the zigzag rows in 1-4a, apparent mainly in empty states, and the shift in the position of the bright spot away from the adatom in empty states of 1-4b above 0.9 eV. Both structures show only one main bright spot and as such can be easily distinguished from the other structures.

Almost all of the adatom structures show partial occupancy at the Fermi level (apart from 1-2b and 1-3); this reflects the bonding of these structures which leaves a half-filled dangling bond at the surface. The two structures which do not show this are more distorted and it is clear that the cost of rearranging bonds has been balanced by the movement of surface states away from the Fermi level.

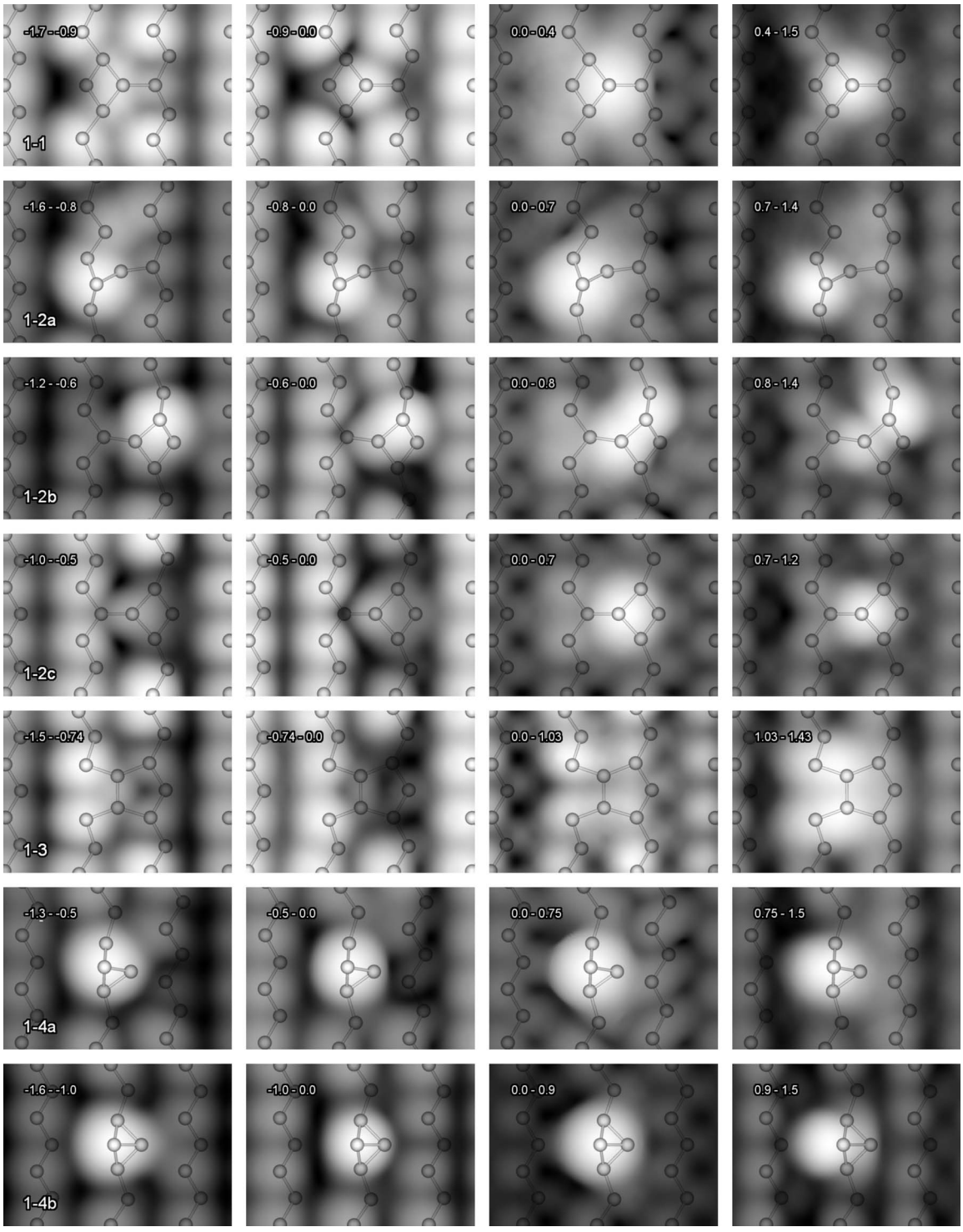

FIG. 6. STM/CITS images of the adsorbed atom on the different stable sites on the (1×1) reconstruction.

2. *The* (2×1) *surface*

The DOS of the complexes on the (2×1) reconstruction (Fig. 7) shows that the adatoms cause attenuation of peaks close to the Fermi level. The 2-1 structure has large peaks in occupied states, below −0.3 eV, while the 2-2 structure has a large peak in empty states, above 0.5 eV. They can also be easily distinguished from their CITS images (Fig. 8) because of their relative position to the ridges of the zigzag rows: the adatom in 2-1 sits on top of a bright line formed by the two rows with a narrow gap in between, whereas the adatom in 2-2 is in between these bright lines. In addition, the adatom in 2-1 appears as a very bright spot both in occupied and empty states and the row distortion can be seen in images close to the Fermi level. In contrast, the adatom in 2-2 does not appear brighter than the surrounding lines and the zigzag rows are not distorted. The physical structures of the two

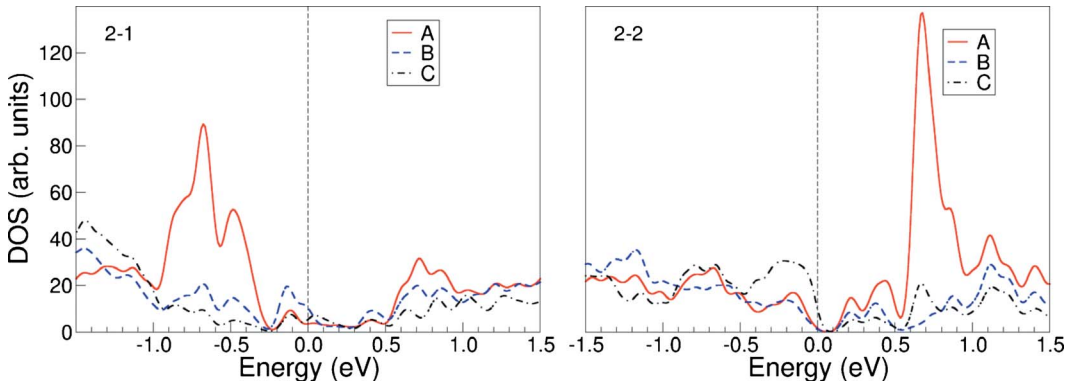

FIG. 7. (Color online) Density of states projected on atoms at the two stable sites on the (2×1) reconstruction.

adatoms go some way to explaining their electronic structure: the 2-1 site is physically higher, leading to brightness in the CITS images, while the 2-2 site is bonded to the second layer in the zigzag chains and is physically significantly lower. This site is also close to planar, which will push the hybridization toward sp^2 with an empty p_z orbital (as seen in the empty states). This planar structure is rather similar to the 1-2b and 1-2c structures on the (1×1) surface, with similar DOS resulting.

D. Si adatom diffusion

1. Diffusion on the (1×1) *surface*

We will first focus on the energy barriers between the less stable configurations and the more stable ones. The energy barrier to stabilize the 1-2c structure by shifting one row is only 0.18 eV. The energy barrier between the 1-4a and 1-2a configurations is 0.20 eV. The movement of the adatom and of a surface atom during the transition is shown in the top left part of Fig. 9. From the 1-2a configuration, it then takes 0.41 eV to reach the 1-1 adsorption site. As can be seen in Fig. 9 (bottom left), atom B of 1-2a moves to the position of the adatom in 1-1 and the original adatom replaces a surface atom.

The transition from 1-2c to 1-1 can already be considered as diffusion along the *b* direction (i.e., along the zigzag rows). The energy barrier is 0.74 eV. As can be seen from the top right part of Fig. 9, diffusion along the zigzag rows can, but does not need to, proceed via configuration 1-2c. The saddle point on the PES is between the 1-2c and 1-1 sites and the energy barrier height (1.09 eV) is independent of whether the end points of the diffusion are 1-1 or 1-2c. An exchange mechanism in diffusion along the direction of the rows is provided by the transition between structures 1-1 to 1-3 to 1-1 further along the row. Here a surface atom (atom B in 1-1) moves in between the zigzag rows to become atom B in 1-3 and forms a dimer with the adatom (atom A both in 1-1 and 1-3), resulting in 1-3. To form the 1-1 structure again but shifted along the zigzag row, atom A moves to the now vacant surface position and atom B effectively becomes the new adatom (Fig. 9, bottom right). The energy barrier on the path from 1-3 to 1-1 is 0.66 eV with respect to the total energy of 1-3 or 1.10 eV with respect to the total energy of 1-1. Simple diffusion and diffusion by an exchange mechanism thus have the same energy barrier.

From inspection of the PES it appears highly unlikely that a path for simple diffusion exists across the rows. Indeed we have not found such a path. There is, however, the possibility of an exchange mechanism from 1-1 to 1-1 (Fig. 9, middle), in which atom D in 1-1 is displaced by the adatom A; in the resulting structure the original adatom A is a surface atom and the original surface atom D is the new adatom. The energy barrier for this transition mechanism is 1.09 eV, the same as for diffusion along rows. The adatom diffusion at the (1×1) reconstruction is therefore equally likely to proceed

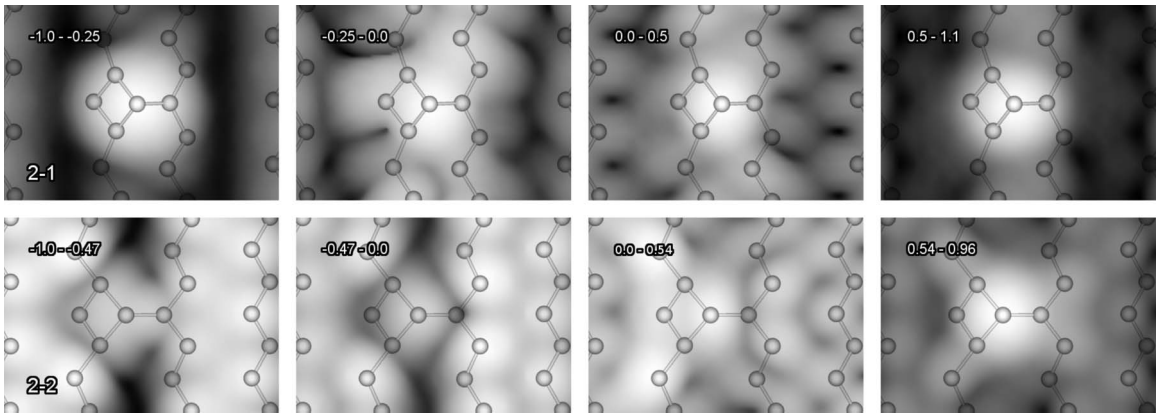

FIG. 8. STM/CITS images of the adsorbed atom on the two stable sites on the (2×1) reconstruction.

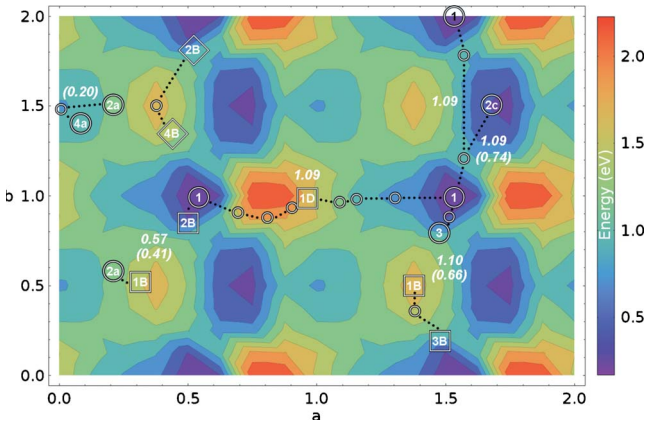

FIG. 9. (Color online) Diffusion of a Si atom on the (1×1) surface shown on the calculated PES (Fig. 2). Large circles show the position of the adatom, with the label corresponding to the label of the system (1- is omitted). Squares represent surface atoms involved in an exchange mechanism and diamonds a surface atom that has significantly moved in the transition. Atom labeling is the same as in Fig. 3. Small circles show the position of the atoms along the transition paths. Dotted lines are drawn only to guide the eye. Numbers in italics give energy barriers (in eV) with respect to the total energy of the 1-1 system. Numbers in brackets give energy barriers (in eV) with respect to the total energy of the less stable of the initial and final configurations. A (2×2) surface unit cell is shown.

along and across the zigzag rows.

2. Diffusion on the (2×1) surface

On the (2×1) surface diffusion from a 2-1 to another 2-1 site, i.e., along the zigzag rows and effectively above the surface, has an energy barrier of 0.50 eV. Diffusion from 2-2 to 2-2, along zigzag rows but at the height of the surface atoms, has a higher energy barrier, 0.95 eV. The energy barrier for diffusion across rows, from 2-2 to 2-1, is 0.51 eV with respect to the total energy of the structure 2-2. The energy barrier that an adatom diffusing from a 2-1 site to another 2-1 site across rows has to overcome is therefore 0.88 eV. We have not found any exchange mechanisms. Diffusion along rows is easier than across rows on the (2×1). In comparison to the (1×1) surface, however, the adatom mobility is higher in either direction. This may well result from the smaller number of stable sites on the (2×1) surface, giving less trapping and making it easier to move the adatom.

3. Comparison to diffusion on the Si(001) surface

The most relevant silicon surface for comparison to Si(110) is Si(001): both surfaces show rows [dimer rows on Si(001) and zigzag rows on Si(110)] giving asymmetry; also, atomic layer epitaxy on Si(001) can lead to nanostructures with Si(110) sidewalls. The $c(4\times2)$ Si(001) surface consists of rows of dimers, spaced 7.7 Å apart, separated by troughs. The preferred direction for diffusion for adatoms is along the rows, with a calculated energy barrier of 0.34 eV (DFT/PW91, Ref. 32). However, the most stable adsorption site is not directly in the diffusion path; the barrier for the adatom to leave the most stable site has been experimentally estimated to be between 0.56 and 0.67 eV (Refs. 33 and 34) and calculated to be 0.6–0.7 eV.[32,35]

Diffusing adatoms will form dimers on top of either the dimer rows or the trough; these dimers diffuse with larger barriers (1.08 or 1.27 eV along the row or trough[36,37]). Diffusion on the Si(001) surface for adatoms is then easier than on both (1×1) and (2×1) Si(110) surfaces [0.6–0.7 eV compared to ~1.1 eV on the (1×1) surface or 0.88 eV on the (2×1) surface]. On Si(001) and (2×1) Si(110) diffusion along rows is favored, while the (1×1) Si(110) surface shows diffusion along and across rows to be energetically equivalent, giving isotropic diffusion. Despite the larger barriers for isolated adatoms on Si(110), the dimerization of adatoms arising from the geometry of Si(001) may well make the diffusion rates on both surfaces similar at higher coverages. Epitaxial growth may therefore proceed at slightly lower temperatures on the Si(001) surface than on either of the Si(110) reconstructions investigated in this work, though this will depend on the rate of deposition and substrate temperatures.

We also consider the likely implications for ALE, where hydrogen lithography is used to create pattern on hydrogen-terminated Si(001), followed by layer-by-layer growth of using gas sources (silane or disilane). The implications are that diffusion of silicon adatoms on Si(110) sidewalls of nanostructures will be activated at temperatures similar to those used for Si(001) epitaxy; crucially, the barriers to diffusion are rather lower than those for hydrogen desorption, so controlled growth will be possible without damage to the passivating hydrogen layer.

IV. CONCLUSIONS

We have comprehensively investigated Si adatom adsorption and diffusion on the (1×1) and (2×1) reconstructions of the Si(110) surface, using density functional theory with the gradient-corrected PBE functional and periodic boundary conditions. On the (1×1) reconstruction three areas of the surface offer stable adsorption sites. There are two possible adsorption sites at the (2×1) reconstruction. At both surfaces the most stable structures are with the adatom adsorbed between two zigzag rows, bound to one atom from one row and two atoms from the other. Several complexes can be stabilized by a lateral shift of one or both zigzag rows, or by a distortion of one row; these different structures can be identified by their DOS and CITS images, which we have provided.

The adatom diffusion on the (1×1) reconstruction is equally likely to proceed along and across the zigzag rows, giving isotropic diffusion on an anisotropic substrate. Along rows either simple diffusion or diffusion via an exchange with one of the surface atoms can occur, with a barrier of 1.09 eV. Across rows only an exchange mechanism is viable. Diffusion on the (2×1) reconstruction has lower energy barriers along the rows than across (0.50 and 0.88 eV, respectively) and no exchange mechanism has been found. The adatom mobility is always higher than on the (1×1) recon-

struction. Study of both Si adsorption and diffusion shows that it is relatively easy to disturb the zigzag rows of the simple reconstructions of the Si(110) surface: this surface shows a tendency to distort, as seen in the complex (5×8) and (16×2) reconstructions observed experimentally.

ACKNOWLEDGMENTS

We would like to thank Graeme Henkelman, Kazushi Miki, and John Randall for helpful discussions. The calculations were done as part of the Grand Challenge program at the University College London High Performance Computing cluster, at the High-End Computing Terascale Resource (HECToR), through the UKCP Consortium, under Grant No. EP/F036884, and at the UCL London Centre for Nanotechnology HPC service. The work was funded by the UK EPSRC Grant No. EP/G024812.

*v.brazdova@ucl.ac.uk
†david.bowler@ucl.ac.uk

[1] S. Sugawa, I. Ohshima, H. Ishino, Y. Saito, M. Hirayama, and T. Ohmi, *IEEE International Electron Devices Meeting Technical Digest, Washington, D.C., December 2001* (IEEE, Piscataway, NJ, 2001), pp. 37.3.1–37.3.4.
[2] Y. Suda, N. Hosoya, and D. Shiratori, J. Cryst. Growth **237-239**, 1404 (2002).
[3] Y. Suda, N. Hosoya, and K. Miki, Appl. Surf. Sci. **216**, 424 (2003).
[4] Y. Yamamoto, Surf. Sci. **313**, 155 (1994).
[5] Y. Yamamoto, Phys. Rev. B **50**, 8534 (1994).
[6] A. J. Hoeven, E. J. Dijkkamp, E. J. van Loenen, and P. J. G. M. van Hooft, Surf. Sci. **211-212**, 165 (1989).
[7] H. Ampo, S. Miura, K. Kato, Y. Ohkawa, and A. Tamura, Phys. Rev. B **34**, 2329 (1986).
[8] Y. Yamamoto, T. Sueyoshi, T. Sato, and M. Iwatsuki, Surf. Sci. **466**, 183 (2000).
[9] W. E. Packard and J. D. Dow, Phys. Rev. B **55**, 15643 (1997).
[10] T. An, M. Yoshimura, I. Ono, and K. Ueda, Phys. Rev. B **61**, 3006 (2000).
[11] K. Sakamoto, M. Setvin, K. Mawatari, P. E. J. Eriksson, K. Miki, and R. I. G. Uhrberg, Phys. Rev. B **79**, 045304 (2009).
[12] N. D. Kim, Y. K. Kim, C.-Y. Park, H. W. Yeom, H. Koh, E. Rotenberg, and J. R. Ahn, Phys. Rev. B **75**, 125309 (2007).
[13] A. A. Stekolnikov, J. Furthmüller, and F. Bechstedt, Phys. Rev. B **70**, 045305 (2004).
[14] A. A. Stekolnikov, J. Furthmüller, and F. Bechstedt, Phys. Rev. Lett. **93**, 136104 (2004).
[15] M. Menon, N. N. Lathiotakis, and A. N. Andriotis, Phys. Rev. B **56**, 1412 (1997).
[16] N. Takeuchi, Surf. Sci. **494**, 21 (2001).
[17] J. P. Perdew, K. Burke, and M. Ernzerhof, Phys. Rev. Lett. **77**, 3865 (1996).
[18] G. Kresse and J. Hafner, Phys. Rev. B **48**, 13115 (1993).
[19] G. Kresse and J. Furthmüller, Phys. Rev. B **54**, 11169 (1996).
[20] P. E. Blöchl, Phys. Rev. B **50**, 17953 (1994).
[21] G. Kresse and D. Joubert, Phys. Rev. B **59**, 1758 (1999).
[22] H. J. Monkhorst and J. D. Pack, Phys. Rev. B **13**, 5188 (1976).
[23] J. Tersoff and D. R. Hamann, Phys. Rev. B **31**, 805 (1985).
[24] G. Henkelman, B. P. Uberuaga, and H. Jónsson, J. Chem. Phys. **113**, 9901 (2000).
[25] D. Sheppard, R. Terrell, and G. Henkelman, J. Chem. Phys. **128**, 134106 (2008).
[26] G. Henkelman and H. Jónsson, J. Chem. Phys. **111**, 7010 (1999).
[27] Y. Tateyama, T. Ogitsu, K. Kusakabe, and S. Tsuneyuki, Phys. Rev. B **54**, 14994 (1996).
[28] J. Klimes, D. R. Bowler, and A. Michaelides, J. Phys.: Condens. Matter **22**, 074203 (2010).
[29] C. R. Hubbard, H. E. Swanson, and F. A. Mauer, J. Appl. Crystallogr. **8**, 45 (1975).
[30] E. Massa, G. Mana, U. Kuetgens, and L. Ferroglio, New J. Phys. **11**, 053013 (2009).
[31] The binding energy E_b is defined as $E_{\mathrm{ads}}-E_{\mathrm{clean}}-E_{\mathrm{Si}}$, where E_{ads}, E_{clean}, and E_{Si} are the total energies of the system with the adsorbed atom, the clean surface, and a gas phase Si atom, respectively. A negative binding energy means that energy is gained upon adsorption.
[32] A. P. Smith and H. Jónsson, Phys. Rev. Lett. **77**, 1326 (1996).
[33] R. A. Wolkow, Phys. Rev. Lett. **74**, 4448 (1995).
[34] Y.-W. Mo, J. Kleiner, M. B. Webb, and M. G. Lagally, Surf. Sci. **268**, 275 (1992).
[35] T. Yamasaki, T. Uda, and K. Terakura, Phys. Rev. Lett. **76**, 2949 (1996).
[36] C. M. Goringe and D. R. Bowler, Phys. Rev. B **56**, R7073 (1997).
[37] B. Borovsky, M. Krueger, and E. Ganz, Phys. Rev. B **59**, 1598 (1999).